Inorganic Chemistry

Article

pubs.acs.org/IC

Synthesis, Structure, and Electrochemistry of the Ni–Au Carbonyl Cluster $[Ni_{12}Au(CO)_{24}]^{3-}$ and Its Relation to $[Ni_{32}Au_6(CO)_{44}]^{6-}$

Iacopo Ciabatti,[†] Cristina Femoni,[†] Maria Carmela Iapalucci,[†] Giuliano Longoni,[†] Stefano Zacchini,[†,*] Serena Fedi,[‡] and Fabrizia Fabrizi de Biani[‡]

[†]Dipartimento di Chimica Fisica e Inorganica, Università di Bologna, Viale Risorgimento 4 - 40136 Bologna, Italy

[‡]Dipartimento di Chimica, Università di Siena, Via De Gasperi 2, Siena, Italy

Supporting Information

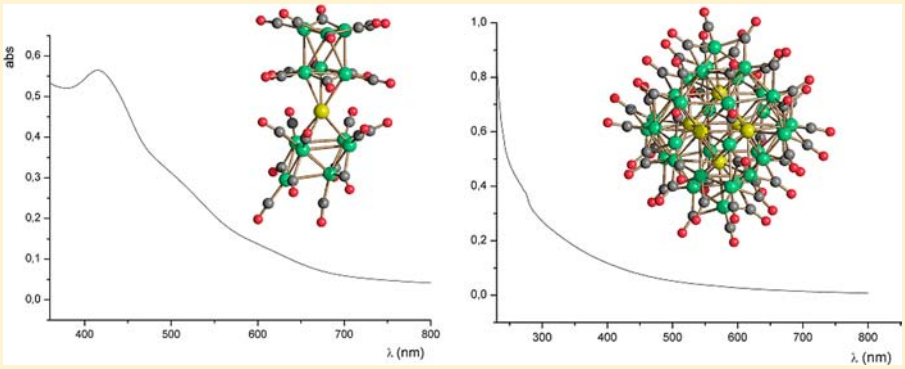

ABSTRACT: A detailed study of the reaction between $[Ni_6(CO)_{12}]^{2-}$ and $[AuCl_4]^-$ afforded the isolation of the new Ni–Au cluster $[Ni_{12}Au(CO)_{24}]^{3-}$ as well as identifying an improved synthesis for the previously reported $[Ni_{32}Au_6(CO)_{44}]^{6-}$. The new $[Ni_{12}Au(CO)_{24}]^{3-}$ cluster is composed by two $[Ni_6(CO)_{12}]^{2-}$ moieties coordinated to a central Au(I) ion, as determined by X-ray diffraction. It is noteworthy that the two $[Ni_6(CO)_{12}]^{2-}$ fragments display different geometries, i.e., trigonal antiprismatic (distorted octahedral) and distorted trigonal prismatic (monocapped square pyramidal). The chemical reactivity of these clusters and their electrochemical behavior have been studied. $[Ni_{12}Au(CO)_{24}]^{3-}$ is irreversibly transformed, upon electrochemical reduction, into Au(0) and $[Ni_6(CO)_{12}]^{2-}$, followed by the reversible reduction of the latter homometallic cluster. Conversely, $[Ni_{32}Au_6(CO)_{44}]^{6-}$ displays five reductions, with apparent features of reversibility, confirming the ability of larger metal carbonyl clusters to reversibly accept and release electrons.

1. INTRODUCTION

We have recently reported the synthesis and crystal structures of the $[Au_{22}Fe_{12}(CO)_{48}]^{6-}$, $[Au_{21}Fe_{10}(CO)_{40}]^{5-}$, $[Au_{28}Fe_{14}(CO)_{52}]^{8-}$, and $[Au_{34}Fe_{14}(CO)_{50}]^{10-}$[1] molecular clusters, which may be viewed as gold nanoclusters stabilized by the $Fe(CO)_4$ and $Fe(CO)_3$ organometallic fragments. In this respect, the $[Ni_{32}Au_6(CO)_{44}]^{6-}$[2] and $[Ni_{12}Au_6(CO)_{24}]^{2-}$[3] molecular clusters reported by Dahl represent the first examples of such an organometallic approach to gold nanoparticles. In fact, they both contain a Au_6 octahedral core stabilized by a $Ni_{32}(CO)_{44}$ shell and four $Ni_3(CO)_6$ triangular units, respectively.

Gold nanoclusters are one of the hottest topics in the recent scientific literature and play a fundamental role in both nanosciences and nanotechnology.[4−8] Several applications for gold nanoclusters are envisioned in chemistry, catalysis, optics, sensing, biology, and medicine among the others.[4−11] Gold nanoclusters are usually stabilized by thiolate or phosphine ligands.[12−19] Thus, the use of organometallic fragments to stabilize them may be viewed as an additional approach to gold cluster chemistry.

Moreover, from a molecular point of view, the structure of $[Ni_{32}Au_6(CO)_{44}]^{6-}$ (Figure 1) is rather interesting, since it contains six fully interstitial Au atoms. As shown by the comparison between the metal frameworks of $[Ni_{32}Au_6(CO)_{44}]^{6-}$ (Figure 1(a)) and that of both $[Pt_{38}(CO)_{44}]^{2-}$[20] (Figure 1(b)) and the iso-structural $[H_2Ni_{24}Pt_{14}(CO)_{44}]^{4-}$,[21] the two differ mainly in the top and bottom layers which in the first is a μ_3-capped ν_2-Ni_6 triangle, while in the second is a Ni_7 centered hexagon. Both these iso-nuclear frameworks are surrounded by a shell of 44 carbonyl groups. The rearrangement from (b) to (a) causes the loss of 6 M-M contacts (6 Ni–Ni in $[Ni_{32}Au_6(CO)_{44}]^{6-}$). Probably as a consequence, $[Ni_{32}Au_6(CO)_{44}]^{6-}$ features 6 and 10 additional cluster valence electrons with respect to $[H_2Ni_{24}Pt_{14}(CO)_{44}]^{4-}$ and $[Pt_{38}(CO)_{44}]^{2-}$, respectively.

It was of interest to verify whether the structural conversion (a)→(b) could occur upon oxidation of $[Ni_{32}Au_6(CO)_{44}]^{6-}$, in view of the fact that it would only require sinking of the capping

Received: July 31, 2012
Published: October 25, 2012

   dx.doi.org/10.1021/ic301679h | Inorg. Chem. 2012, 51, 11753–11761

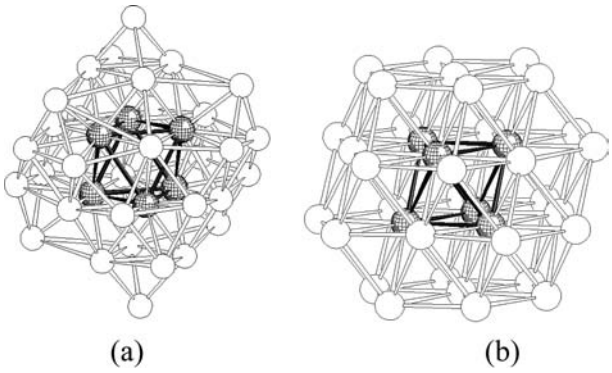

Figure 1. Metal frameworks of (a) $[Ni_{32}Au_6(CO)_{44}]^{6-2}$ and (b) $[Pt_{38}(CO)_{44}]^{2-20}$ (very loose Ni−Ni contacts up to ca. 3.5 Å have been included in the drawing of the former for sake of clarity).

atoms in the centers of the ν_2 triangles with their swelling to give centered hexagons. Moreover, we also wished to investigate the chemical and electrochemical properties of $[Ni_{32}Au_6(CO)_{44}]^{6-}$ in order to verify if interstitial Au-atoms are able to induce multivalence in molecular carbonyl clusters, as previously found for interstitial Ag, Ni, Pt, and Rh atoms.[22]

Herein, we report an improved synthesis of $[Ni_{32}Au_6(CO)_{44}]^{6-}$ together with the synthesis and structural characterization of the new $[Ni_{12}Au(CO)_{24}]^{3-}$ cluster. Their chemical and electrochemical properties have been investigated and are also reported in detail. Finally, their different electronic properties have been tested by means of UV−visible spectroscopy and extended Hückel molecular orbital (EHMO) calculations.

2. RESULTS AND DISCUSSION

2.1. Synthesis of $[NEt_4]_3[Ni_{12}Au(CO)_{24}]$. The very interesting $[Ni_{32}Au_6(CO)_{44}]^{6-}$ cluster was originally obtained by L. F. Dahl in low yields by reacting $Au(PPh_3)Cl$, $Ni(OAc)_2$, and $[Ni_6(CO)_{12}]^{2-}$ (molar ratio 1:3:2) in dmso for 2 days.[2] Its formation was accompanied by other unidentified Au−Ni carbonyl clusters. In view of the peculiar structure of $[Ni_{32}Au_6(CO)_{44}]^{6-}$, it was of interest to obtain it in larger yields in order to study its chemical and electrochemical properties. Moreover, the presence of side products during its synthesis suggested the possibility of obtaining new Au−Ni carbonyl clusters. Thus, we have investigated the reaction of miscellaneous salts of $[Ni_6(CO)_{12}]^{2-}$ with $[AuCl_4]^-$ in acetone, by adding increasing amounts of the Au(III) complex to the Ni carbonylate solution, and following the reaction *via* FT-IR. The highest yields of the target compound were obtained using *ca.* 0.9 mols of $[AuCl_4]^-$ per mole of $[Ni_6(CO)_{12}]^{2-}$, in accord to eq 1:

$$7[Ni_6(CO)_{12}]^{2-} + 6[AuCl_4]^- \rightarrow [Ni_{32}Au_6(CO)_{44}]^{6-} + 5Ni^{2+} + 5Ni(CO)_4 + 20CO + 24Cl^- \quad (1)$$

The compound was purified by removing the solvent *in vacuo*, washing the solid residue with water, toluene, thf, and acetone, and extraction of pure $[Ni_{32}Au_6(CO)_{44}]^{6-}$ in CH_3CN [ν(CO): 2012(m), 1889(vs) cm^{-1}]. Yields as high as 54% (based on Au) were obtained. During the work up, the presence of a new carbonyl species with ν(CO) at 2010(vs), 1986(sh), and 1822(ms) was obtained from the acetone extraction. This new species becomes the major product by decreasing the amount of Au(III), i.e. 0.6−0.8 mols of $[AuCl_4]^-$ per mole of $[Ni_6(CO)_{12}]^{2-}$. This improved synthesis allowed the isolation and structural characterization of the new cluster, which was $[Ni_{12}Au(CO)_{24}]^{3-}$ as determined by single crystal X-ray diffraction on its $[NEt_4]_3[Ni_{12}Au(CO)_{24}]$ salt. Its formation can be explained following eq 2, which requires 0.67 mols of $[AuCl_4]^-$ per mole of $[Ni_6(CO)_{12}]^{2-}$ in a rather good agreement with the experiments:

$$6[Ni_6(CO)_{12}]^{2-} + 4[AuCl_4]^- \rightarrow 2[Ni_{12}Au(CO)_{24}]^{3-} + 2Au + 3Ni^{2+} + 16Cl^- + 9Ni + 24CO \quad (2)$$

In detail, $[NEt_4][AuCl_4]$ is added in small portions to an acetone solution of $[NEt_4]_2[Ni_6(CO)_{12}]$, and the solvent was removed *in vacuo* after two hours. The residue is washed with water, toluene, and thf, and the crude product extracted in acetone. Crystals suitable for X-ray analysis of $[NEt_4]_3[Ni_{12}Au(CO)_{24}]$ were obtained by slow diffusion of isopropyl alcohol over the acetone solution. Since eqs 1 and 2 require relatively

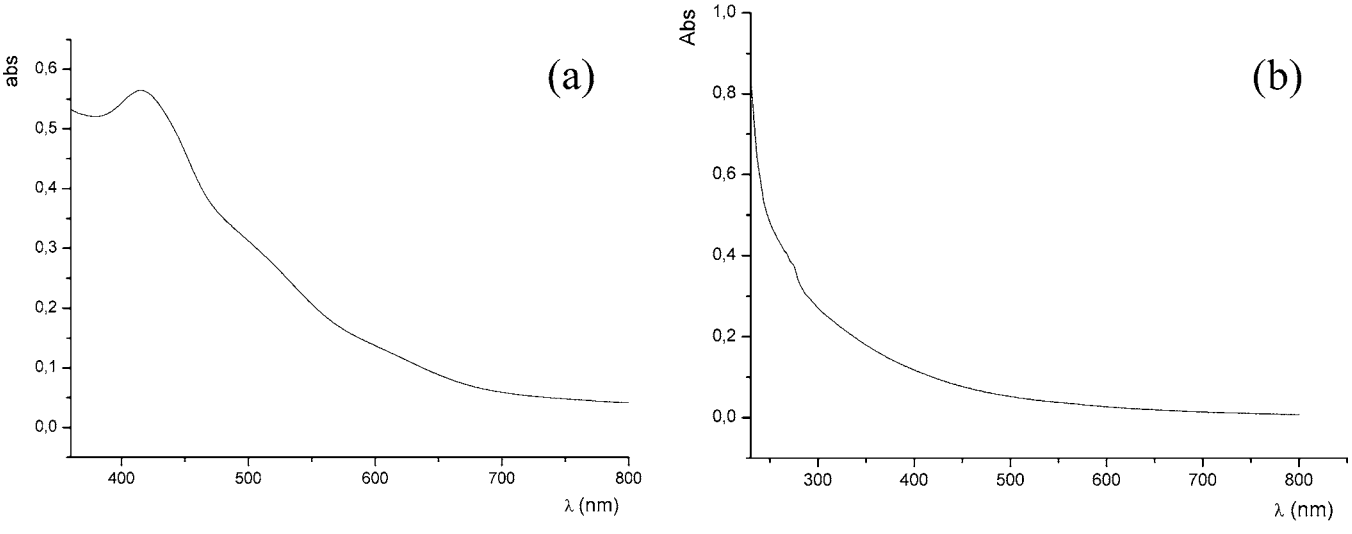

Figure 2. UV−visible spectra of (a) $[Ni_{12}Au(CO)_{24}]^{3-}$ (10^{-5} M in acetone) and (b) $[Ni_{32}Au_6(CO)_{44}]^{6-}$ (10^{-5} M in CH_3CN).

dx.doi.org/10.1021/ic301679h | *Inorg. Chem.* 2012, 51, 11753−11761

similar ratios of the reagents, the formation of $[Ni_{12}Au(CO)_{24}]^{3-}$ is always accompanied by small amounts of $[Ni_{32}Au_6(CO)_{44}]^{6-}$. Nonetheless, the two products can be easily separated since the former is soluble in acetone and the latter only in CH_3CN. The yields of $[Ni_{12}Au(CO)_{24}]^{3-}$ based on Ni (*ca.* 40%) and Au (*ca.* 25%) are not very high, but this is easily explained by considering eq 2.

The two clusters display distinct FT-IR (see above) and electronic spectra (Figure 2). In particular, $[Ni_{12}Au(CO)_{24}]^{3-}$ shows a strong absorption at 416 nm, whereas $[Ni_{32}Au_6(CO)_{44}]^{6-}$ displays a nearly featureless spectrum with a small shoulder at *ca.* 274 nm. These different electronic spectra are in keeping with the different nuclearities of these clusters. Thus, the smaller $[Ni_{12}Au(CO)_{24}]^{3-}$ shows a molecular-like spectrum (Figure 2(a)), whereas $[Ni_{32}Au_6(CO)_{44}]^{6-}$ displays an UV–visible spectrum (Figure 2(b)) similar to those of small metal nanoparticles.[23]

In agreement with eqs 1 and 2, $[Ni_{12}Au(CO)_{24}]^{3-}$ is converted into $[Ni_{32}Au_6(CO)_{44}]^{6-}$ after addition of further $[AuCl_4]^-$.

$[Ni_{12}Au(CO)_{24}]^{3-}$ is thermally unstable. In fact, after refluxing in acetone under N_2 atmosphere, it is completely converted into a mixture of $[Ni_{32}Au_6(CO)_{44}]^{6-}$, $[Ni_6(CO)_{12}]^{2-}$, and $Ni(CO)_4$ in agreement with eq 3:

$$6[Ni_{12}Au(CO)_{24}]^{3-} \xrightarrow{\Delta} [Ni_{32}Au_6(CO)_{44}]^{6-} + 6[Ni_6(CO)_{12}]^{2-} + 4Ni(CO)_4 + 12CO \quad (3)$$

Similarly, $[Ni_{12}Au(CO)_{24}]^{3-}$ reacts with HBF_4 yielding $[Ni_{32}Au_6(CO)_{44}]^{6-}$ and $Ni(CO)_4$, as the only carbonyl products, in accord to eq 4:

$$6[Ni_{12}Au(CO)_{24}]^{3-} + 12H^+ \rightarrow [Ni_{32}Au_6(CO)_{44}]^{6-} + 25Ni(CO)_4 + 15Ni + 6H_2 \quad (4)$$

In addition, the oxidation of $[Ni_{12}Au(CO)_{24}]^{3-}$ with $[C_7H_7][BF_4]$ affords, once again, $[Ni_{32}Au_6(CO)_{44}]^{6-}$ which is further oxidized to $[Ni_{32}Au_6(CO)_{44}]^{5-}$ (see below and Section 2.3).

Conversely, by treating an acetone solution of $[Ni_{12}Au(CO)_{24}]^{3-}$ under CO (1 atm) at room temperature, $[Ni_5(CO)_{12}]^{2-}$ and $Ni(CO)_4$ are formed as the only carbonyl products. Solid Au metal is also formed as indicated by the appearance of a gold mirror on the surface of the reaction flask. A possible stoichiometry for the reaction is suggested by eq 5. Indeed, as described in Section 2.2, $[Ni_{12}Au(CO)_{24}]^{3-}$ may be viewed as a complex composed by two $[Ni_6(\mu\text{-}CO)_6(CO)_6]^{2-}$ ligands coordinated to a central Au^+ ion, and the CO-induced conversion of $[Ni_6(\mu\text{-}CO)_6(CO)_6]^{2-}$ to $[Ni_5(CO)_{12}]^{2-}$ and $Ni(CO)_4$ is a well-known process.[24]

$$2[Ni_{12}Au(CO)_{24}]^{3-} + 12CO \rightarrow 4[Ni_5(CO)_{12}]^{2-} + 3Ni(CO)_4 + 2Au + Ni^{2+} \quad (5)$$

In agreement with the above hypothesis, $[Ni_{12}Au(CO)_{24}]^{3-}$ is converted into $[Ni_6(CO)_{12}]^{2-}$ after addition of an excess of Br^- ions. This reaction is likely to be a nucleophilic substitution where the two $[Ni_6(CO)_{12}]^{2-}$ coordinated to Au(I) in $[Ni_{12}Au(CO)_{24}]^{3-}$ are replaced by two bromide ions, as schematized in eq 6. Indeed, $[AuBr_2]^-$ is known to be a rather stable Au(I) complex.[25]

$$[Ni_{12}Au(CO)_{24}]^{3-} + 2Br^- \rightarrow 2[Ni_6(CO)_{12}]^{2-} + [AuBr_2]^- \quad (6)$$

The availability in good yields of $[Ni_{32}Au_6(CO)_{44}]^{6-}$ from reaction 1 as well as reactions 3 and 4 prompted an investigation of its chemical behavior. First of all, as already suggested by its isolation from reaction 4 and at difference from most Ni–Pt polyanions,[26] $[Ni_{32}Au_6(CO)_{44}]^{6-}$ is not protonated by acids. Conversely, it is similarly prone to redox changes as other large metal carbonyl clusters.[22] Thus, $[Ni_{32}Au_6(CO)_{44}]^{6-}$ [ν(CO) 2012(m), 1889(vs) cm^{-1} in dmf] is stepwise reduced to $[Ni_{32}Au_6(CO)_{44}]^{7-}$ [ν(CO) 1989(m), 1875(vs) cm^{-1} in dmf] and $[Ni_{32}Au_6(CO)_{44}]^{8-}$ [ν(CO) 1972(m), 1869(vs) cm^{-1} in dmf] by addition of Na/naphthalene in dmf. These reductions are chemically reversed by mild oxidizing agents. In view of the very negative potentials at which the reductions occur (see Section 2.3), water is already a suitable oxidant, and, thus, all attempts to isolate the reduced species failed. In fact, while trying to recover $[Ni_{32}Au_6(CO)_{44}]^{n-}$ (n = 7, 8) from the dmf solutions by addition of aqueous $[NEt_4]Br$, $[Ni_{32}Au_6(CO)_{44}]^{6-}$ was always obtained as the final product. Contrarily to initial expectations, $[Ni_{32}Au_6(CO)_{44}]^{6-}$ is only oxidized to a purported unstable $[Ni_{32}Au_6(CO)_{44}]^{5-}$ [ν(CO): 2020(m), 1897(vs) cm^{-1} in CH_3CN] by means of $[C_7H_7][BF_4]$. Addition of this oxidizing agent in excess only led to complete decomposition.

$[Ni_{32}Au_6(CO)_{44}]^{6-}$ reacts with carbon monoxide, eventually resulting in the formation of $Ni(CO)_4$ and Au metal. This decomposition process might be appealing since it seems to open the possibility of producing Au or Au–Ni clusters, rather than a gold mirror, once carried out in the presence of suitable ligands. Interestingly in the initial steps of the above degradation reaction the intermediate formation of a species showing IR absorptions very close to those of $[Ni_{12}Au_6(CO)_{24}]^{2-}$ could be observed. In spite of some efforts, we have been unable to stop the reaction at this stage and isolate this compound.

2.2. Crystal Structure of $[NEt_4]_3[Ni_{12}Au(CO)_{24}]$. The crystal structure of $[NEt_4]_3[Ni_{12}Au(CO)_{24}]$ has been determined by X-ray crystallography (Figure 3 and Table 1). The asymmetric unit of the unit cell contains one cluster anion and three $[NEt_4]^+$ cations (all located on general positions). The $[Ni_{12}Au(CO)_{24}]^{3-}$ cluster anion can be described as being composed of two $[Ni_6(\mu\text{-}CO)_6(CO)_6]^{2-}$ units coordinated to a central Au^+ cation. It is remarkable that the two $[Ni_6(\mu\text{-}CO)_6(CO)_6]^{2-}$ units display different structures and coordination modes to the Au(I) center (Figure 4).

Thus, the $[Ni_6(\mu\text{-}CO)_6(CO)_6]^{2-}$ unit comprising Ni(1) to Ni(6) (Figure 4(a)) adopts the usual trigonal antiprismatic (distorted octahedral) structure previously found in the parent $[Ni_6(\mu\text{-}CO)_6(CO)_6]^{2-}$ free dianion.[24,27] As for the free dianion, this $[Ni_6(\mu\text{-}CO)_6(CO)_6]^{2-}$ unit contains six terminal CO ligands (one per Ni atom) and six μ-CO bridging the six edges of the two triangular bases of the trigonal antiprism. Conversely, the intertriangular Ni–Ni contacts are not bridged by any CO. As a consequence, the intratriangular Ni–Ni contacts [2.3773(16)-2.3919(18) Å; average 2.385(4) Å] in the coordinated trigonal antiprismatic $[Ni_6(\mu\text{-}CO)_6(CO)_6]^{2-}$ unit are considerably shorter than the intertriangular ones [2.7468(18)-2.8016(18) Å; average 2.768(4) Å] as also found in the free $[Ni_6(\mu\text{-}CO)_6(CO)_6]^{2-}$ dianion [average intratriangular 2.37 Å; average intertriangular 2.77 Å]. This unit is

dx.doi.org/10.1021/ic301679h | *Inorg. Chem.* 2012, 51, 11753–11761

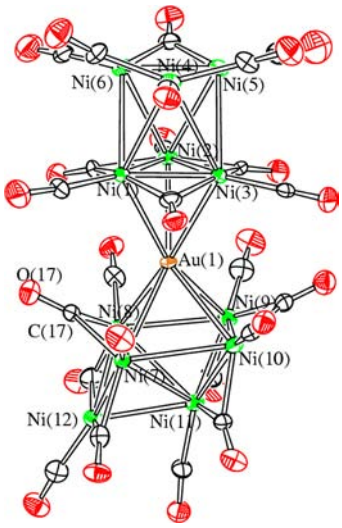

Figure 3. Molecular structure of $[Ni_{12}Au(CO)_{24}]^{3-}$ with key atoms labeled. Thermal ellipsoids are at the 50% probability level (Ni, green; Au, orange; C, black; O, red).

Table 1. Metal–Metal Contacts (Å) for $[NEt_4]_3[Ni_{12}Au(CO)_{24}]$

bond	length	bond	length
Au(1)–Ni(1)	2.7158(12)	Au(1)–Ni(2)	2.7455(14)
Au(1)–Ni(3)	2.7115(13)		
Au(1)–Ni(7)	2.7338(12)	Au(1)–Ni(8)	2.6805(14)
Au(1)–Ni(9)	2.7068(14)	Au(1)–Ni(10)	2.6669(13)
Ni(1)–Ni(2)	2.3773(16)	Ni(1)–Ni(3)	2.3841(17)
Ni(1)–Ni(4)	2.7532(18)	Ni(1)–Ni(6)	2.7714(18)
Ni(2)–Ni(3)	2.3795(18)	Ni(2)–Ni(6)	2.7468(18)
Ni(2)–Ni(5)	2.7833(18)	Ni(3)–Ni(5)	2.7542(18)
Ni(3)–Ni(4)	2.8016(18)	Ni(4)–Ni(5)	2.3895(18)
Ni(4)–Ni(6)	2.3919(18)	Ni(5)–Ni(6)	2.387(2)
Ni(7)–Ni(8)	2.4092(19)	Ni(7)–Ni(12)	2.4619(18)
Ni(7)–Ni(11)	2.7143(17)	Ni(7)–Ni(10)	2.7811(18)
Ni(8)–Ni(12)	2.4417(19)	Ni(8)–Ni(11)	2.7964(18)
Ni(8)–Ni(9)	2.8463(19)	Ni(9)–Ni(10)	2.3795(19)
Ni(9)–Ni(11)	2.4066(18)	Ni(10)–Ni(11)	2.4041(18)
Ni(11)–Ni(12)	2.6168(18)		

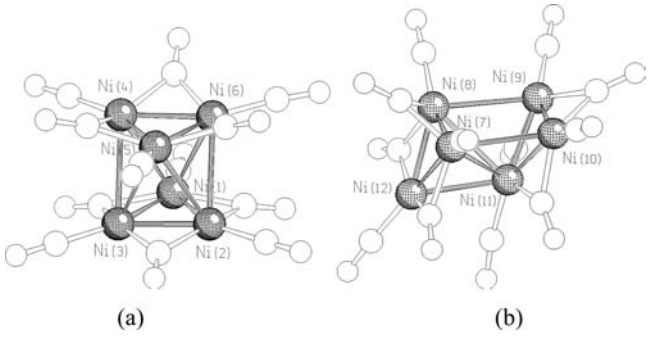

Figure 4. The two different $[Ni_6(\mu\text{-}CO)_6(CO)_6]^{2-}$ units contained in $[Ni_{12}Au(CO)_{24}]^{3-}$.

coordinated to Au(1) *via* a Ni_3 face, which is known to possess the character of a soft Lewis base.[28]

The second $[Ni_6(\mu\text{-}CO)_6(CO)_6]^{2-}$ unit (Figure 4(b)) can be viewed as a distorted square pyramid comprising Ni(7) to Ni(11) which is capped on the triangular Ni(7)–Ni(8)–Ni(11) face by Ni(12). This unit is coordinated to Au(1) through the square base of the pyramid, i.e., Ni(7), Ni(8), Ni(9), and Ni(10). Alternatively, this Ni_6 framework may be described as a distorted trigonal prism, coordinated to Au(1) *via* a lateral square face and having the remaining two square faces heavily compressed along a diagonal. As a consequence, whereas in the described above trigonal antiprismatic $[Ni_6(\mu\text{-}CO)_6(CO)_6]^{2-}$ unit there were twelve Ni–Ni contacts at bonding distances, in this distorted trigonal prismatic unit there are only eleven contacts at bonding distances. It is noteworthy that in a regular trigonal prismatic Ni_6 cage there would be only nine edges; the two additional bonds herein present are due to compression along corresponding diagonals in two of the three lateral square faces. The presence of 11 Ni–Ni bonds is also in agreement with the description of this Ni_6 unit as a monocapped square pyramid.

Also in this unit there are six terminal CO (one per Ni atom) and six μ-CO bridging the edges of the two triangular bases of the trigonal prism. As expected, the CO-bridged intratriangular Ni–Ni contacts [2.3795(19)-2.4619(18) Å; average 2.417(5)Å] are significantly shorter than the unbridged intertriangular distances [2.6168(18)-2.8463(19) Å; average 2.751(4) Å].

The central Au atom displays seven Au–Ni contacts, three with a triangular face of the trigonal antiprismatic $[Ni_6(\mu\text{-}CO)_6(CO)_6]^{2-}$ unit [2.7115(13)-2.7455(14) Å; average 2.724(2) Å], and four with the uncompressed square face of the distorted trigonal prismatic $[Ni_6(\mu\text{-}CO)_6(CO)_6]^{2-}$ unit [2.6669(13)-2.7338(12) Å; average 2.698(3) Å]. These values compare well with the Au–Ni contacts found in $[Ni_{32}Au_6(CO)_{44}]^{6-2}$ and $[Ni_{12}Au_6(CO)_{24}]^{2-}$.[3] Moreover, the μ-CO(17) ligand bridging Ni(7)–Ni(8) is bent toward Au(1) [C(17)···Au(1) 2.747(8) Å] as a consequence of the square face being coordinated to gold.

The angle formed between Au and the centroids of the Ni_3 and Ni_4 faces is 173.77(2)°, in agreement with the classical digonal coordination of Au(I).[29] A similar situation was found in $[Pt_6Au(CO)_6(PMe_3)_4]^+$, where the central Au^+ cation was coordinated to two triangular $[Pt(\mu\text{-}CO)_3(PMe_3)_4]$ units.[30]

The only previous example in which a soft Lewis acid is coordinated to an intact $[Ni_6(CO)_{12}]^{2-}$ unit is represented by $\{Cd_2Cl_3[Ni_6(CO)_{12}]_2\}^{3-}$ in which a $Cd_2Cl_3^+$ group is coordinated to the triangular faces of two slightly distorted trigonal prismatic $[Ni_6(CO)_{12}]^{2-}$ units.[31] The present case, thus, shows two further geometries for coordinated $[Ni_6(CO)_{12}]^{2-}$ units, i.e. trigonal antiprismatic (as in the free cluster) and monocapped square pyramidal (heavily distorted trigonal prismatic). This indicates that the $[Ni_6(CO)_{12}]^{2-}$ unit is rather flexible and can easily change its structure after coordination to a metallic site. Further examples of hexanuclear Ni_6-cages acting as Lewis bases toward cationic centers are found in Ni–In clusters, *viz.* $[Ni_6(\mu_3\text{-}InBr_3)(\eta^2\text{-}\mu_3\text{-}In_2Br_5)(CO)_{11}]^{3-}$, $[Ni_6(\eta^2\text{-}\mu_3\text{-}In_2Br_5)_2(CO)_{10}]^{4-}$, and $[Ni_{12}(\mu_6\text{-}In)(\eta^2\text{-}\mu_3\text{-}In_2Br_4OH)(CO)_{22}]^{4-}$.[32] Nonetheless, in all these cases, the original $[Ni_6(CO)_{12}]^{2-}$ unit loses one or two CO ligands formally resulting in $[Ni_6(CO)_{11}]^{4-}$ and $[Ni_6(CO)_{10}]^{6-}$ species stabilized by coordination to various $InBr_3$, $[In_2Br_5]^+$, and $[In_2Br_4OH]^+$ fragments or naked In^{3+} ions. Interestingly, also in these Ni–In clusters, the Ni_6 cage displays different geometries, such as distorted octahedral, trigonal antiprismatic, and monocapped square pyramid. In particular, $[Ni_{12}(\mu_6\text{-}In)(\eta^2\text{-}\mu_3\text{-}In_2Br_4OH)(CO)_{22}]^{4-}$ as the herein reported $[Ni_{12}Au$-

dx.doi.org/10.1021/ic301679h | *Inorg. Chem.* 2012, 51, 11753–11761

$(CO)_{24}]^{3-}$ cluster contains two geometrically different Ni_6 units.

2.3. Electrochemistry of $[Ni_{12}Au(CO)_{24}]^{3-}$ and $[Ni_{32}Au_6(CO)_{44}]^{6-}$. As it is shown by the cyclic voltammogram in Figure 5, the trianion $[Ni_{12}Au(CO)_{24}]^{3-}$ undergoes both cathodic and anodic processes, which will be discussed separately.

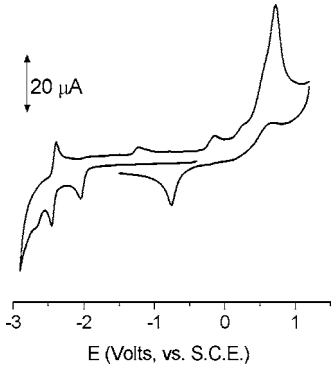

Figure 5. Cyclic voltammogram recorded at a gold electrode in thf solution of $[NBu_4]_3[Ni_{12}Au(CO)_{24}]$ (1.5×10^{-3} M). $[NBu_4][PF_6]$ (0.2 M) supporting electrolyte. Scan rate 0.2 V s^{-1}.

In the cathodic region, it undergoes a chemically irreversible reduction at −2.01 V, followed by a chemically reversible reduction at −2.42 V. This latter process is observed at the same potential for the free $[Ni_6(CO)_{12}]^{2-}$ cluster. Therefore, a reasonable interpretation is that an ECE process occurs during the reduction of $[Ni_{12}Au(CO)_{24}]^{3-}$ as schematized in Scheme 1. Overall, it is likely that $[Ni_{12}Au(CO)_{24}]^{3-}$ is irreversibly reduced at −2.01 V to Au(0) and $[Ni_6(CO)_{12}]^{2-}$, followed by the reversible reduction of the latter at −2.42 V.

Scheme 1

$$[Ni_{12}Au(CO)_{24}]^{3-} \xrightarrow[-2.01\ V]{+1e^-} [Ni_{12}Au(CO)_{24}]^{4-} \longrightarrow 2[Ni_6(CO)_{12}]^{2-} + Au$$

$$[Ni_6(CO)_{12}]^{2-} \underset{-2e^-}{\overset{+2e^-}{\rightleftharpoons}} [Ni_6(CO)_{12}]^{4-}$$

In agreement with this hypothesis, the frontier region of the EHMO diagram (in the −11 to −9 eV interval of energy), calculated with CACAO,[33] for $[Ni_{12}Au(CO)_{24}]^{3-}$ (Figure 6) displays a rather large HOMO−LUMO gap (0.785 eV), and the LUMO (MO 122) receives contributions only from the two $[Ni_6(CO)_{12}]^{2-}$ moieties. Thus, it is likely that, after reduction, the additional electron is delocalized over these Ni-CO units destabilizing the formal $[Ni_{12}Au(CO)_{24}]^{4-}$ adducts, which, in turn, undergoes an internal reduction to Au metal and $[Ni_6(CO)_{12}]^{2-}$.

The process described in Scheme 1 has been confirmed by a bulk electrolysis experiment. In fact, the quantitative reduction (E_w = −2.2 V) of the sample makes the brown solution of $[Ni_{12}Au(CO)_{24}]^{3-}$ to turn red, as expected for a solution of $[Ni_6(CO)_{12}]^{2-}$, while the peak at −2.01 V progressively disappears without altering the reduction process at −2.42 V. Such a behavior is clearly illustrated in Figure 7 in which the Osteryoung square wave voltammograms of the sample before and after the bulk electrolysis are compared.

To unquestionably establish the nature of the product obtained after the irreversible reduction of $[Ni_{12}Au(CO)_{24}]^{3-}$,

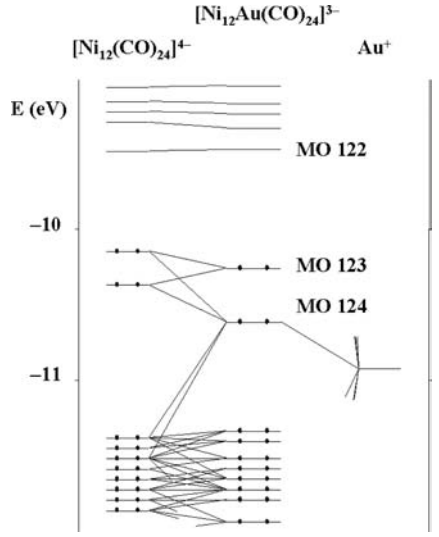

Figure 6. Frontier region (in the −11 to −9 eV interval of energy) of the EHMO diagram of $[Ni_{12}Au(CO)_{24}]^{3-}$.

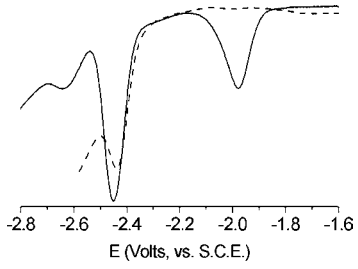

Figure 7. Osteryoung square-wave voltammograms recorded at a gold electrode in a thf solution of $[Ni_{12}Au(CO)_{24}]^{3-}$ before (full line) and after (dashed line) exhaustive electrolysis at E_w = −2.2 V. $[NBu_4][NPF_6]$ supporting electrolyte (0.2 M). Scan rates: 0.1 V s^{-1}.

the redox process has been monitored step-by-step by IR *ex-situ* spectroelectrochemistry. As it is shown in Figure 8, the gradual

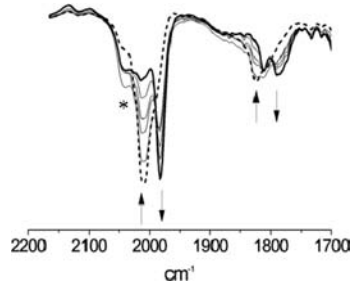

Figure 8. IR ex-situ spectroelectrochemistry showing the evolution of the probing ν(CO) stretching, from the original sample (dotted line) to the exhaustively electrolyzed one (full line), throughout the step-by-step reduction of $[Ni_{12}Au(CO)_{24}]^{3-}$.

disappearance of the ν(CO) bands at 2010(vs), 1986(sh), and 1822(ms) cm^{-1}, characteristic of the original trianion in thf solution, is accompanied by the appearance of bands at 1983(vs), 1810(m), and 1792(m) cm^{-1}, which are typical of a pristine sample of $[Ni_6(CO)_{12}]^{2-}$.

The production of $[Ni_6(CO)_{12}]^{2-}$ throughout the reduction of $[Ni_{12}Au(CO)_{24}]^{3-}$ is not quantitative and is accompanied by the formation of side products such as the volatile complex

dx.doi.org/10.1021/ic301679h | *Inorg. Chem.* 2012, 51, 11753−11761

$Ni(CO)_4$, as indicated by the transient appearance of the peak at 2038 cm^{-1} indicated by an asterisk in Figure 8.

The features of the cathodic region of the cyclic voltammogram of $[Ni_{12}Au(CO)_{24}]^{3-}$ are more than evocative of what has been observed in the case of $\{Cd_2Cl_3[Ni_6(CO)_{12}]_2\}^{3-}$ and prompted a reinvestigation of the redox behavior of this latter, as well as that of the dianions $[Ni_6(CO)_{12}]^{2-}$ and $[Ni_9(CO)_{18}]^{2-}$. In fact, in the paper describing the redox behavior of $\{Cd_2Cl_3[Ni_6(CO)_{12}]_2\}^{3-}$,[31] a reversible reduction at −2.43 V was reported as also preceded by an ill-resolved irreversible peak, formerly interpreted as the sign of the presence of impurities. Anyway, in the light of the present findings, a different interpretation appears to be more consistent. Really, once compared, as for the cathodic region in Figure 9, the cyclic voltammograms of this family of clusters

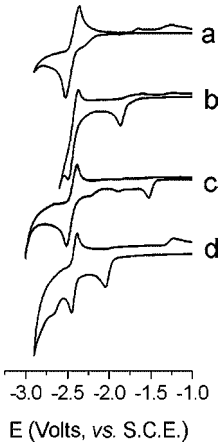

Figure 9. Cyclic voltammograms recorded at a gold electrode in thf solution of (a) $[Ni_6(CO)_{12}]^{2-}$; (b) $[Ni_9(CO)_{18}]^{2-}$; (c) $\{Cd_2Cl_3[Ni_6(CO)_{12}]_2\}^{3-}$; (d) $[Ni_{12}Au(CO)_{24}]^{3-}$. Normalized currents of samples in mM concentration. $[NBu_4][PF_6]$ (0.2 M) supporting electrolyte. Scan rate 0.2 V s^{-1}.

clearly reveal their relationships and may suggest that in all cases the one-electron irreversible reduction of $[X\text{-}\{Ni_6(CO)_{12}\}_2]^{3-}$ (E_p = −2.01 V for X = Au, E_p= −1.52 V for X = Cd_2Cl_3) involves the detachment of the X unit connecting two $[Ni_6(CO)_{12}]^{2-}$ clusters, which subsequently undergo the expected reduction at about −2.42 V. Similarly, the irreversible reduction (E_p = −1.86 V) of $[Ni_9(CO)_{18}]^{2-}$, which is synthetically obtained by oxidation of $[Ni_6(CO)_{12}]^{2-}$, is rapidly followed by the quantitative reformation of this latter, indicating the reversibility of the reaction 7:

$$2[Ni_9(CO)_{18}]^{2-} + 2e^- \rightleftarrows 3[Ni_6(CO)_{12}]^{2-} \quad (7)$$

This interpretation of the redox behavior of this family of clusters is also consistent with the acid−base interaction existing between the soft Lewis base $[Ni_6(CO)_{12}]^{2-}$ and the acid fragment X^+. In fact, this interaction is broken as soon as the acidity of X^+ is switched off by reduction.

As in the previous work, the very negative cathodic value of the unique reversible process prevented any reliable coulometric determination of the number of electrons involved in this redox processes. Anyway, as it shown in Figure 10, the second derivative of the Osteryoung square wave voltammograms indicates that, in all cases, the reversible reduction at about −2.42 V, erroneously described as monoelectronic, actually involves the subsequent addition of two-electrons.

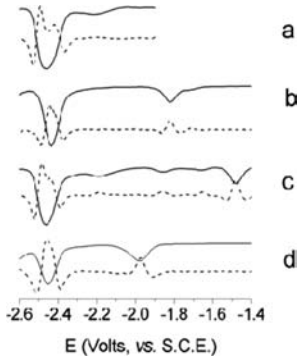

Figure 10. Osteryoung square-wave voltammograms (full line) and its second derivative (dashed line) recorded at a gold electrode in a thf solution of (a) $[Ni_6(CO)_{12}]^{2-}$; (b) $[Ni_9(CO)_{18}]^{2-}$; (c) $\{Cd_2Cl_3[Ni_6(CO)_{12}]_2\}^{3-}$; (d) $[Ni_{12}Au(CO)_{24}]^{3-}$. $[NBu_4][NPF_6]$ supporting electrolyte (0.2 M). Scan rates: 0.1 V s^{-1}.

Finally, it may be noteworthy that a very similar behavior has been observed in the anodic region for all these compounds, which, after an unresolved multielectronic oxidation at ∼+0.7 V generate a new, unidentified product which is reduced at −0.75 V. An attempt to unambiguously identify this latter by IR spectroelectrochemistry performed on $[Ni_{12}Au(CO)_{24}]^{3-}$ had only modest success since the main difference between the IR spectrum of the original solution and that obtained after bulk electrolysis (E_w = +0.72 V) is the appearance of a strong signal at 2038 cm^{-1}, indicating the presence $Ni(CO)_4$. As a matter of fact, the electrolysis of $[Ni_{12}Au(CO)_{24}]^{3-}$ makes a brown powder to deposit on the electrode, so it is possible that the main product of the oxidation process is not detected by the IR technique.

Turning on the redox behavior of the larger $[Ni_{32}Au_6(CO)_{44}]^{6-}$, it is, as expected, very different from that observed for the previously described class of low nuclearity clusters. In fact, the hexa-anion undergoes five reductions at −0.74 V, −1.06 V, −1.30 V, −1.58 V, and −1.80 V, with apparent features of reversibility and two irreversible oxidations at −0.36 and −0.18 V (Figure 11). The peaks/current ratio

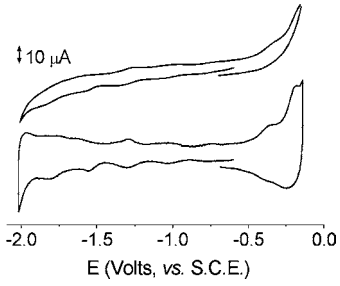

Figure 11. Cyclic voltammogram (top) and deconvoluted cyclic voltammogram (bottom) recorded at a platinum electrode in acetonitrile solution of $[NBu_4]_6[Ni_{32}Au_6(CO)_{44}]$, ($1.1 \times 10^{-3}$ M). $[NBu_4][PF_6]$ (0.2 M) supporting electrolyte. Scan rate 0.2 V s^{-1}.

would suggest that the number of electrons involved in the oxidations and in the third and forth reductions could be the double of those involved in the first two reductions. Anyway, the low concentration obtained with this heavy cluster, which has also the property to foul the electrodes, as indicated by the fact that the signals are detected only with a platinum working electrode and with no other electrode material, deprives of true

dx.doi.org/10.1021/ic301679h | Inorg. Chem. 2012, 51, 11753−11761

reliability any reasoning on the current intensity. Interestingly, all the redox processes are almost equally spaced by ~259 mV, which is a classic trait of interstitial clusters with this structural features. This value can be compared with the values of 400 and 300 mV, respectively, displayed by $[Pt_{38}(CO)_{44}]^{2-}$,[20] $[H_2Ni_{24}Pt_{14}(CO)_{44}]^{4-}$,[21] and $[HNi_{38}Pt_6(CO)_{48}]^{5-}$ which contain an encapsulated octahedron of Pt atoms and display an identical or slightly superior nuclearity.[26]

It is noteworthy that $[Ni_{32}Au_6(CO)_{44}]^{6-}$ (Figure 12) displays a rather small HOMO−LUMO gap (0.196 eV), as usually

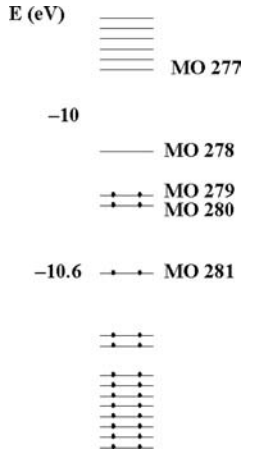

Figure 12. Frontier region (in the −11.5 to −9.5 eV interval of energy) of the EHMO diagram of $[Ni_{32}Au_6(CO)_{44}]^{6-}$.

found for multivalent metal carbonyl clusters (MCCs).[22] Moreover, the propensity of $[Ni_{32}Au_6(CO)_{44}]^{6-}$ to be oxidized and reduced shown by these electrochemical experiments is in good agreement with its chemical behavior described in Section 2.1.

3. CONCLUSIONS

The new $[Ni_{12}Au(CO)_{24}]^{3-}$ cluster described in this paper represents an intermediate of the synthesis of $[Ni_{32}Au_6(CO)_{44}]^{6-}$ starting from $[Ni_6(CO)_{12}]^{2-}$ and $[AuCl_4]^-$. The two clusters considerably differ in their structures and properties.

From a structural point of view, $[Ni_{12}Au(CO)_{24}]^{3-}$ may be viewed as a Lewis acid−base adduct composed by a central Au^+ ion and two $[Ni_6(CO)_{12}]^{2-}$ carbonylate ligands. Interestingly, this represents the second example in which an intact $[Ni_6(CO)_{12}]^{2-}$ anion acts as soft Lewis base.[31] Moreover, the two $[Ni_6(CO)_{12}]^{2-}$ anions coordinated to Au^+ assume different geometries, suggesting the large flexibility of the metal cores of metal carbonyl clusters.

Conversely, $[Ni_{32}Au_6(CO)_{44}]^{6-}$, previously described by Dahl,[2] is composed by an octahedral Au_6 core completely surrounded by a Ni_{32} cage and, thus, may be viewed as a molecular core−shell nanocluster.

Even the properties of these two Au−Ni carbonyl clusters are rather different, in part because $[Ni_{32}Au_6(CO)_{44}]^{6-}$ is far more stable than $[Ni_{12}Au(CO)_{24}]^{3-}$, the latter being easily converted into the former. Moreover, their electrochemical behaviors are rather significant. $[Ni_{12}Au(CO)_{24}]^{3-}$ is irreversibly reduced to Au(0) and $[Ni_6(CO)_{12}]^{2-}$, whereas decomposition is mainly observed after electrochemical oxidation. These observations confirm that, in the absence of *ad hoc* conditions, small carbonyl clusters tend to be electron precise, and, thus, they are destabilized after addition or subtraction of electrons.[22] Conversely, $[Ni_{32}Au_6(CO)_{44}]^{6-}$ is multivalent, in the sense that it undergoes several reversible redox processes, and, therefore, it may be viewed as a molecular nanocapacitor.[22] As a matter of fact, its electrochemical behavior is similar to the ones reported for other high nuclearity metal carbonyl clusters, confirming that the appearance of multivalence in large clusters is a general phenomenon which may be taken as a proof of the incipient metallization of their metal cores.

The different electronic status of $[Ni_{12}Au(CO)_{24}]^{3-}$ and $[Ni_{32}Au_6(CO)_{44}]^{6-}$ is also evidenced by their UV−visible spectra, which show a strong (molecular-like) absorption for the former and an almost featureless profile for the latter, reminiscent of the electronic spectra of small metal nanoparticles.[23]

It seems, therefore, safe to conclude that "*real*" Au(0) is at least as effective as Pt in inducing multivalence and driving the molecular carbonyl cluster core toward transition in the metallic state. Comparable values of ΔE between consecutive redox couples in the 260−400 mV range have also been reported for $Au_{144}(SR)_{60}$,[34] even if the nuclearity of this gold nanocluster stabilized by thiolates is more than three times that of the Ni−Au, Ni−Pt, and Pt carbonyl clusters described here, viz., $[Ni_{32}Au_6(CO)_{44}]^{6-}$, $[H_2Ni_{24}Pt_{14}(CO)_{44}]^{4-}$, and $[Pt_{38}(CO)_{44}]^{2-}$. Such a delayed metallization of the gold thiolate finds justification in our earlier suggestion that these Au nanocluster consist of a positively charged core of Au atoms, featuring a nuclearity well inferior than implicated by the formula, which are stabilized by negative $[Au_n(SR)_{n+1}]^-$ anions behaving as 4-e donor. In such a view, the structurally characterized $Au_{25}(SR)_{18}$ and $Au_{38}(SR)_{24}$[12,13] will respectively contain only 8 and 14 Au(0), whereas the purported $Au_{144}(SR)_{60}$[34,35] may end up in containing only 60−80 Au(0). These heavily reduced nuclearities make these two distinct families of clusters (carbonyl and thiolate clusters) fairly comparable not only in their electronic configuration (viz. electron count) but also in their properties (viz. metallization with nuclearity).

4. EXPERIMENTAL SECTION

4.1. General Procedures. All reactions and sample manipulations were carried out using standard Schlenk techniques under nitrogen and in dried solvents. All the reagents were commercial products (Aldrich) of the highest purity available and used as received, except $[NEt_4]_2[Ni_6(CO)_{12}]$ which has been prepared according to the literature.[24,27] Analysis of Ni and Au were performed by atomic absorption on a Pye-Unicam instrument. Analyses of C, H, and N were obtained with a ThermoQuest FlashEA 1112NC instrument. IR spectra were recorded on a Perkin-Elmer SpectrumOne interferometer in CaF_2 cells. Structure drawings have been performed with SCHAKAL99.[36]

Cyclic voltammetry was performed in a three-electrode cell containing a platinum or gold working electrode surrounded by a platinum-spiral counter electrode and an aqueous saturated calomel reference electrode (SCE) mounted with a Luggin capillary. A BAS 100W electrochemical analyzer was used as the polarizing unit. All the potential values are referred to the saturated calomel electrode (SCE). Under the present experimental conditions, the one-electron oxidation of ferrocene occurs at E° = +0.59 V in thf solution and at E° = +0.39 V in acetonitrile solution. Controlled potential coulometry was performed in an H-shaped cell with anodic and cathodic compartments separated by a sintered-glass disk. The working macroelectrode was a platinum gauze, and a mercury pool was used as the counter electrode. Anhydrous 99.9% HPLC-grade acetonitrile and tetrahydrofuran (Aldrich) have been distilled before use. Fluka $[NBu_4][PF_6]$

Table 2. Crystal Data and Experimental Details for $[NEt_4]_3[Ni_{12}Au(CO)_{24}]$

	$[NEt_4]_3[Ni_{12}Au(CO)_{24}]$
formula	$C_{48}H_{60}AuN_3Ni_{12}O_{24}$
Fw	1964.48
T, K	100(2)
λ, Å	0.71073
crystal system	trigonal
space group	$P3_2$
a, Å	*12.4728(7)*
b, Å	12.4728(7)
c, Å	36.243(2)
cell volume, Å^3	4883.0(5)
Z	3
D_c, g cm^{-3}	2.004
μ, mm^{-1}	5.699
F(000)	2928
crystal size, mm	0.23 × 0.13 × 0.11
θ limits, °	1.12−25.02
index ranges	$-14 \le h \le 14$
	$-14 \le k \le 14$
	$-43 \le l \le 43$
reflections collected	46786
independent reflections	11500 [R_{int} = 0.0654]
completeness to θ max	100.0%
data/restraints/parameters	11500/363/796
goodness on fit on F^2	1.076
R_1 ($I > 2\sigma(I)$)	0.0354
wR_2 (all data)	0.0858
largest diff. peak and hole, e Å^{-3}	3.282/−0.633

(electrochemical grade) was used as supporting electrolytes. Infrared (IR) *ex-situ* spectroelectrochemical measurements were carried out using a Perkin-Elmer FT-IR System SPECTRUM BX spectrophotometer and a SPECAC universal transmission cell for the analysis of liquids equipped with CaF_2 windows.

Warning: *CO and Ni(CO)$_4$ may be generated during manipulation of these compounds.*

4.2. Synthesis of $[NEt_4]_3[Ni_{12}Au(CO)_{24}]$. Solid $[NEt_4][AuCl_4]$ (0.89 g, 1.90 mmol) was added in small portions to an acetone (30 mL) solution of $[NEt_4]_2[Ni_6(CO)_{12}]$ (2.21 g, 2.33 mmol) over a period of 1 h. The solution was stirred at room temperature for a further hour, and, then, the solvent removed *in vacuo*. The residue was washed with water (40 mL), toluene (40 mL), and thf (20 mL). The crude product was extracted in acetone (20 mL), and crystals suitable for X-ray analysis were obtained by slow diffusion of isopropyl alcohol (40 mL) over the acetone solution of the product (yields 0.92 g, 24.7% based on Au, 40.2% based on Ni).

$C_{48}H_{60}AuN_3Ni_{12}O_{24}$ (1964.48): calcd. C 29.35, H 3.08, N 2.14, Ni 35.86, Au 10.03; found: C 29.48, H 2.92, N 2.26, Ni 35.99, Au 9.89. IR (acetone, 293 K) ν(CO): 2010(vs), 1986(sh), and 1822(ms) cm^{-1}. IR (nujol, 293 K) ν(CO): 1995(vs), 1833(sh), 1815(ms), 1775(m) cm^{-1}.

4.3. Synthesis of $[NEt_4]_6[Ni_{32}Au_6(CO)_{44}]$. Solid $[NEt_4][AuCl_4]$ (1.04 g, 2.22 mmol) was added in small portions to an acetone (30 mL) solution of $[NEt_4]_2[Ni_6(CO)_{12}]$ (2.21 g, 2.33 mmol) over a period of 1 h. The solution was stirred at room temperature for a further hour, and, then, the solvent was removed *in vacuo*. The residue was washed with water (40 mL), toluene (40 mL), thf (20 mL), and acetone (20 mL). The crude product was extracted in CH_3CN (20 mL), and a microcrystalline powder of $[NEt_4]_6[Ni_{32}Au_6(CO)_{44}]$ was obtained after addition of di-iso-propyl-ether (50 mL) (yields 0.87 g, 54.2% based on Au, 39.2% based on Ni).

$C_{92}H_{120}Au_6N_6Ni_{32}O_{44}$ (5073.94): calcd. C 21.78, H 2.38, N 1.66, Ni 37.02, Au 23.29; found: C 21.86, H 2.20, N 1.54, Ni 36.81, Au 23.06. IR (CH_3CN, 293 K) ν(CO): 2012(m), 1889(vs) cm^{-1}.

4.4. X-ray Crystallographic Study. Crystal data and collection details for $[NEt_4]_3[Ni_{12}Au(CO)_{24}]$ are reported in Table 2. The diffraction experiments were carried out on a Bruker APEX II diffractometer equipped with a CCD detector using Mo−Kα radiation. Data were corrected for Lorentz polarization and absorption effects (empirical absorption correction SADABS).[37] Structures were solved by direct methods and refined by full-matrix least-squares based on all data using F^2.[38] Hydrogen atoms were fixed at calculated positions and refined by a riding model. All non-hydrogen atoms were refined with anisotropic displacement parameters.

The asymmetric unit of the unit cell contains one cluster anion and three $[NEt_4]^+$ cations (all located on general positions). The crystals display both merohedral (by a *m* plane) and racemic twinning which have been refined simultaneously using the TWIN 0 1 0 1 0 0 0 0 −1 −4 line in SHELXL and three batch scale factors (BASF). These refined as 0.279(5), 0.289(5), and 0.218(5), respectively, indicating that the twinning involves four components of similar extension. Similar *U* restraints (s.u. 0.005) were applied to the C and O atoms. The thermal ellipsoids of the O-atoms in the carbonyl ligands were restrained to an isotropic-like behavior (ISOR line in SHELXL; s.u. 0.005).

■ ASSOCIATED CONTENT

Ⓢ Supporting Information

CIF file giving X-ray crystallographic data for the structure determination of $[NEt_4]_3[Ni_{12}Au(CO)_{24}]$. This material is available free of charge via the Internet at http://pubs.acs.org.

■ AUTHOR INFORMATION

Corresponding Author

*Fax: +39 0512093690, E-mail: stefano.zacchini@unibo.it.

Notes

The authors declare no competing financial interest.

■ ACKNOWLEDGMENTS

The financial support of MIUR (PRIN2008) and the University of Bologna is gratefully acknowledged. Funding by Fondazione CARIPLO, Project No. 2011-0289, is heartily acknowledged.

■ REFERENCES

(1) Femoni, C.; Iapalucci, M. C.; Longoni, G.; Tiozzo, C.; Zacchini, S. *Angew. Chem., Int. Ed.* **2008**, *137*, 483.

(2) Tran, N. T.; Kawano, M.; Powell, D. R.; Hayashi, R. K.; Campana, C. F.; Dahl, L. F. *J. Am. Chem. Soc.* **1999**, *121*, 5945.

(3) (a) Whoolery, A. J.; Dahl, L. F. *J. Am. Chem. Soc.* **1991**, *113*, 6683. (b) Whoolery Johnson, A. J.; Spencer, B.; Dahl, L. F. *Inorg. Chim. Acta* **1994**, *227*, 269.

(4) (a) Bruchez, M., Jr.; Moronne, M.; Gin, P.; Weiss, S.; Alivisatos, A. P. *Science* **1998**, *281*, 2013. (b) Abid, J. P.; Girault, H. H.; Brevet, P. F. *Chem. Commun.* **2001**, *9*, 829. (c) Templeton, A. C.; Wuelfing, W. P.; Murray, R. W. *Acc. Chem. Res.* **2000**, *33*, 27. (d) Daniel, M.-C.; Astruc, D. *Chem. Rev.* **2004**, *104*, 293. (e) Whetten, R. L.; Shafigullin, M. N.; Khoury, J. T.; Schaaff, T. G.; Vezmar, I.; Alvarez, M. M.; Wilkinson, A. *Acc. Chem. Res.* **1999**, *32*, 397.

(5) (a) Tracy, J. B.; Kalyuzhny, G.; Crowe, M. C.; Balasubramanian, R.; Choi, J.-P.; Murray, R. W. *J. Am. Chem. Soc.* **2007**, *129*, 6706. (b) Price, R. C.; Whetten, R. L. *J. Am. Chem. Soc.* **2005**, *127*, 13750. (c) Shichibu, Y.; Negishi, Y.; Tsukuda, T.; Teranishi, T. *J. Am. Chem. Soc.* **2005**, *127*, 13464. (d) Jin, R. *Nanoscale* **2010**, *2*, 343. (e) Parker, J. F.; Fields-Zinna, C. A.; Murray, R. W. *Acc. Chem. Res.* **2010**, *43*, 1289. (f) Gutel, T.; Santini, C. C.; Philippot, K.; Padua, A.; Pelzer, K.; Chaudret, B.; Chauvin, Y.; Basset, J. M. *J. Mater. Chem.* **2009**, *19*, 3624.

(6) (a) Kreibig, U.; Vollmer, M. *Optical Properties of Metal Clusters*; Springer-Verlag: New York, 1995. (b) Zhu, M.; Eckenhoff, W. T.; Pintauer, T.; Jin, R. *J. Phys. Chem. C* **2008**, *112*, 14221. (c) Zhu, M.; Aikens, C. M.; Hollander, F. J.; Schatz, G. C.; Jin, R. *J. Am. Chem. Soc.* **2008**, *130*, 5883.

(7) (a) Maity, P.; Xie, S.; Yamauchi, M.; Tsukuda, T. *Nanoscale* **2012**, *4*, 4027. (b) Hutchings, G. J.; Brust, M.; Schmidbaur, H. *Chem. Soc. Rev.* **2008**, *37*, 1759. (c) Häkkinen, H. *Chem. Soc. Rev.* **2008**, *37*, 1847. (d) Sperling, R. A.; Rivera Gil, P.; Zhang, F.; Zanella, M.; Park, W. J. *Chem. Soc. Rev.* **2008**, *37*, 1896.
(8) (a) Haruta, M. *Gold Bull.* **2004**, *37*, 27. (b) Huang, J.; Akita, T.; Faye, J.; Fukitani, T.; Takei, T.; Haruta, M. *Angew. Chem., Int. Ed.* **2009**, *48*, 7862. (c) Edwards, J. K.; Solsona, B.; Ntainjua, N. E.; Carley, A. F.; Herzing, A. A.; Kiely, C. J.; Hutchings, G. J. *Science* **2009**, *323*, 1037. (d) Murray, R. W. *Chem. Rev.* **2008**, *108*, 2688.
(9) (a) Haruta, M.; Kobayashi, T.; Sano, H.; Yamada, N. *Chem. Lett.* **1987**, *4*, 405. (b) Hutchings, G. J. *J. Catal.* **1985**, *96*, 292. (c) Haruta, M. *Catal. Today* **1997**, *36*, 153. (d) Hashmi, A. S. K.; Hutchings, G. J. *Angew. Chem., Int. Ed.* **2006**, *45*, 7896.
(10) (a) Chaki, N. K.; Negishi, Y.; Tsunoyama, H.; Shichibu, Y.; Tsukuda, T. *J. Am. Chem. Soc.* **2008**, *130*, 8608. (b) Pei, Y.; Gao, Y.; Zeng, X. C. *J. Am. Chem. Soc.* **2008**, *130*, 7830. (c) Lopez-Acevedo, O.; Akola, J.; Whetten, R. L.; Grönbeck, H.; Häkkinen, H. *J. Phys. Chem. C* **2009**, *113*, 5035. (d) Wang, W.; Murray, R. W. *Langmuir* **2005**, *21*, 7015.
(11) (a) Walter, M.; Akola, J.; Lopez-Acevedo, O.; Jadzinsky, P. D.; Calero, G.; C. Ackerson, J.; Whetten, R. L.; Grönbeck, H.; Häkkinen, H. *Proc. Natl. Acad. Sci. U.S.A.* **2008**, *105*, 9157. (b) Jiang, D. E.; Tiago, M. L.; Luo, W.; Dai, S. *J. Am. Chem. Soc.* **2008**, *130*, 2777.
(12) Heaven, M. W.; Dass, A.; White, P. S.; Holt, K. M.; Murray, R. W. *J. Am. Chem. Soc.* **2008**, *130*, 3754.
(13) Qian, H.; Eckenhoff, W. T.; Zhu, Y.; Pintauer, T.; Jin, R. *J. Am. Chem. Soc.* **2010**, *132*, 8280.
(14) Jadzinsky, P. D.; Calero, G.; Ackerson, C. J.; Bushnell, D. A.; Kornberg, R. D. *Science* **2007**, *318*, 430.
(15) Brust, M.; Walker, M.; Bethell, D.; Schiffrin, D. J.; Whyman, R. *J. Chem. Soc., Chem. Commun.* **1994**, 801.
(16) (a) Whetten, R. L.; Khoury, J. T.; Alvarez, M. M.; Murthy, S.; Vezmar, I.; Wang, Z. L.; Stephens, P. W.; Cleveland, C. L.; Luedtke, W. D.; Landmann, U. *Adv. Mater.* **1996**, *8*, 428. (b) Negishi, Y.; Nobusada, K.; Tsukuda, T. *J. Am. Chem. Soc.* **2005**, *127*, 5261. (c) Shichibu, Y.; Negishi, Y.; Tsunoyama, H.; Kanehara, M.; Teranishi, T.; Tsukuda, T. *Small* **2007**, *3*, 835. (d) Qian, H.; Zhu, Y.; Jin, R. *ACS Nano* **2009**, *3*, 3795.
(17) (a) Das, A. *Nanoscale* **2012**, *4*, 2260. (b) Stellwagen, D.; Weber, A.; Bovenkamp, G. L.; Jin, R.; Bitter, J. H.; Kumar, C. S. S. R. *RSC Adv.* **2012**, *2*, 2276.
(18) (a) Bos, W.; Kanters, R. P. F.; van Halen, C. J.; Bosman, W. P.; Behm, H.; Smits, J. M. M.; Beurskens, P. T.; Bour, J. J.; Pignolet, L. H. *J. Organomet. Chem.* **1986**, *307*, 385. (b) Briant, C. E.; Theobald, B. R. C.; White, J. W.; Bell, L. K.; Mingos, D. M. P. *J. Chem. Soc., Chem. Commun.* **1981**, 201. (c) Teo, B. K.; Shi, X.; Zhang, H. *J. Am. Chem. Soc.* **1992**, *114*, 2743. (d) Schmid, G.; Boese, R.; Pfeil, R.; Bandermann, F.; Meyer, S.; Calis, G. H. M.; Jvan der Velden, W. A. *Chem. Ber.* **1981**, *114*, 3634.
(19) (a) Shichibu, Y.; Knonishi, K. *Small* **2010**, *6*, 1216. (b) Teo, B. K.; Zhang, H.; Shi, X. *Inorg. Chem.* **1994**, *33*, 4086. (c) Mingos, D. M. P. *Chem. Soc. Rev.* **1986**, *15*, 31.
(20) (a) Ceriotti, A.; Masciocchi, N.; Macchi, P.; Longoni, G. *Angew. Chem., Int. Ed.* **1999**, *38*, 3724. (b) Roth, J. D.; Lewis, G. J.; Kiang, X.; Dahl, L. F.; Weaver, M. J. *J. Phys. Chem.* **1992**, *96*, 7219. (c) Femoni, C.; Kaswalder, F.; Iapalucci, M. C.; Longoni, G.; Mehlstaubl, M.; Zacchini, S. *Chem. Commun.* **2005**, 5769.
(21) (a) Femoni, C.; Iapalucci, M. C.; Longoni, G.; Svensson, P. H. *J. Chem. Soc., Chem. Commun.* **2001**, 1776. (b) Femoni, C.; Iapalucci, M. C.; Longoni, G.; Svensson, P. H. *J. Chem. Soc., Chem. Commun.* **2004**, 2274.
(22) (a) Femoni, C.; Iapalucci, M. C.; Kaswalder, F.; Longoni, G.; Zacchini, S. *Coord. Chem. Rev.* **2006**, *250*, 1580. (b) Zacchini, S. *Eur. J. Inorg. Chem.* **2011**, 4125.
(23) (a) Alvarez, M. M.; Khoury, J. T.; Schaaff, T. G.; Shafigullin, M. N.; Vezmar, I.; Whetten, R. L. *J. Phys. Chem. B* **1997**, *101*, 3706. (b) Hostetler, M. J.; Wingate, J. E.; Zhong, C.-J.; Harris, J. E.; Vachet, R. W.; Clark, M. R.; Londono, J. D.; Green, S. J.; Stokes, J. J.; Wignall, G. D.; Glish, G. L.; Porter, M. D.; Evans, N. D.; Murray, R. W. *Langmuir* **1998**, *14*, 17.
(24) (a) Longoni, G.; Chini, P.; Lower, L. D.; Dahl, L. F. *J. Am. Chem. Soc.* **1975**, *97*, 5034. (b) Longoni, G.; Chini, P.; Cavalieri, A. *Inorg. Chem.* **1976**, *15*, 3025.
(25) Braunstein, P. *J. Chem. Soc., Dalton Trans.* **1973**, 1845.
(26) (a) Ceriotti, A.; Demartin, F.; Longoni, G.; Manassero, M.; Marchionna, M.; Piva, G.; Sansoni, M. *Angew. Chem., Int. Ed.* **1985**, *24*, 696. (b) Demartin, F.; Femoni, C.; Iapalucci, M. C.; Longoni, G.; Macchi, P. *Angew. Chem., Int. Ed.* **1999**, *38*, 531. (c) Fabrizi de Biani, F.; Femoni, C.; Iapalucci, M. C.; Longoni, G.; Zanello, P.; Ceriotti, A. *Inorg. Chem.* **1999**, *38*, 3721. (d) Femoni, C.; Iapalucci, M. C.; Longoni, G.; Svensson, P. H.; Zanello, P.; Fabrizi de Biani, F. *Chem.—Eur. J.* **2004**, *10*, 2318.
(27) Calabrese, J. C.; Dahl, L. F.; Cavalieri, A.; Chini, P.; Longoni, G.; Martinengo, S. *J. Am. Chem. Soc.* **1974**, *96*, 2616.
(28) Femoni, C.; Kaswalder, F.; Iapalucci, M. C.; Longoni, G.; Zacchini, S. *Chem. Commun.* **2006**, 2135.
(29) Orgel, L. E. *J. Chem. Soc.* **1958**, 4186.
(30) de Silva, N.; Laufenberg, J. W.; Dahl, L. F. *Chem. Commun.* **2006**, 4437.
(31) Femoni, C.; Iapalucci, M. C.; Longoni, G.; Ranuzzi, F.; Zacchini, S.; Fedi, S.; Zanello, P. *Eur. J. Inorg. Chem.* **2007**, 4064.
(32) Demartin, F.; Iapalucci, M. C.; Longoni, G. *Inorg. Chem.* **1993**, *32*, 5536.
(33) Mealli, C.; Proserpio, D. M. *J. Chem. Educ.* **1990**, *67*, 399.
(34) (a) Qian, H.; Jin, R. *Chem. Mater.* **2011**, *23*, 2209. (b) Quinn, B. M.; Liljeroth, P.; Laaksonen, T.; Kantturi, K. *J. Am. Chem. Soc.* **2003**, *125*, 6644. (c) Ingram, R. S.; Hostetler, M. J.; Murray, R. W.; Schaaff, T. G.; Khoury, J. T.; Whetten, R. L.; Bigioni, T. P.; Guthrie, D. K.; First, P. N. *J. Am. Chem. Soc.* **1997**, *119*, 9279.
(35) (a) Qian, H.; Jin, R. *Nano Lett.* **2009**, *9*, 4083. (b) Fields-Zinna, C. A.; Sardar, R.; Beasley, C. A.; Murray, R. W. *J. Am. Chem. Soc.* **2009**, *131*, 16266.
(36) Keller, E. SCHAKAL99, University of Freiburg, Germany, (1999).
(37) Sheldrick, G. M. *SADABS*, Program for empirical absorption correction, University of Göttingen, Germany, 1996.
(38) Sheldrick, G. M. *SHELX97*, Program for crystal structure determination, University of Göttingen, Germany, 1997.